

RESEARCH ARTICLE

The Semantic Variant of Primary Progressive Aphasia: Clinical and Neuroimaging Evidence in Single Subjects

Leonardo Iaccarino¹, Chiara Crespi^{1,2}, Pasquale Anthony Della Rosa³, Eleonora Catricalà⁴, Lucia Guidi⁴, Alessandra Marcone⁵, Fabrizio Tagliavini⁶, Giuseppe Magnani⁷, Stefano F. Cappa^{4,2}, Daniela Perani^{1,2,3,8*}

1 Vita-Salute San Raffaele University and Division of Neuroscience, San Raffaele Scientific Institute, Milan, Italy, **2** CERMAC, Vita-Salute San Raffaele University, Milan, Italy, **3** Istituto di Bioimmagini e Fisiologia Molecolare C.N.R., Segrate, Italy, **4** Istituto Universitario degli Studi Superiori—IUSS, Pavia, Italy, **5** Department of Clinical Neurosciences, San Raffaele Hospital, Milan, Italy, **6** IRCCS Foundation “Carlo Besta” Neurological Institute, Milan, Italy, **7** Departments of Neurology, San Raffaele Hospital, Milan, Italy, **8** Nuclear Medicine Unit, San Raffaele Hospital, Milan, Italy

* perani.daniela@hsr.it



OPEN ACCESS

Citation: Iaccarino L, Crespi C, Della Rosa PA, Catricalà E, Guidi L, Marcone A, et al. (2015) The Semantic Variant of Primary Progressive Aphasia: Clinical and Neuroimaging Evidence in Single Subjects. *PLoS ONE* 10(3): e0120197. doi:10.1371/journal.pone.0120197

Academic Editor: Stefano L Sensi, University G. D’Annunzio, ITALY

Received: January 3, 2015

Accepted: February 5, 2015

Published: March 10, 2015

Copyright: © 2015 Iaccarino et al. This is an open access article distributed under the terms of the [Creative Commons Attribution License](https://creativecommons.org/licenses/by/4.0/), which permits unrestricted use, distribution, and reproduction in any medium, provided the original author and source are credited.

Data Availability Statement: This is a clinical study and therefore the authors confirm that some access restrictions apply to the data underlying the findings. However, the anonymized dataset will be made available upon request to the corresponding author (D.P.) due to ethical restrictions and patients’ privacy.

Funding: This research was supported by the Italian Ministry of Health. The funders had no role in study design, data collection and analysis, decision to publish, or preparation of the manuscript.

Abstract

Background/Aim

We present a clinical-neuroimaging study in a series of patients with a clinical diagnosis of semantic variant of primary progressive aphasia (svPPA), with the aim to provide clinical-functional correlations of the cognitive and behavioral manifestations at the single-subject level.

Methods

We performed neuropsychological investigations, ¹⁸F-FDG-PET single-subject and group analysis, with an optimized SPM voxel-based approach, and correlation analyses. A measurement of white matter integrity by means of diffusion tensor imaging (DTI) was also available for a subgroup of patients.

Results

Cognitive assessment confirmed the presence of typical semantic memory deficits in all patients, with a relative sparing of executive, attentional, visuo-constructional, and episodic memory domains. ¹⁸F-FDG-PET showed a consistent pattern of cerebral hypometabolism across all patients, which correlated with performance in semantic memory tasks. In addition, a majority of patients also presented with behavioral disturbances associated with metabolic dysfunction in limbic structures. In a subgroup of cases the DTI analysis showed FA abnormalities in the inferior longitudinal and uncinate fasciculi.

Discussion

Each svPPA individual had functional derangement involving an extended, connected system within the left temporal lobe, a crucial part of the verbal semantic network, as well as an

Competing Interests: The authors have declared that no competing interests exist.

involvement of limbic structures. The latter was associated with behavioral manifestations and extended beyond the area of atrophy shown by CT scan.

Conclusion

Single-subject ^{18}F -FDG-PET analysis can account for both cognitive and behavioral alterations in svPPA. This provides useful support to the clinical diagnosis.

Introduction

In the mid-1970s, Endel Tulving proposed the concept of semantic memory [1]. After this insightful work, Elizabeth Warrington reported three patients in which “a selective impairment” of this cognitive function was the prominent clinical finding [2]. A detailed cognitive evaluation of the syndrome of semantic dementia was first provided by Snowden and co-workers in 1989 [3]. Three years later, Hodges et al. described several cases with similar semantic disruption showing circumscribed atrophy of temporal poles (TPs) in 1992 [4]. The syndrome was recognized as one of the clinical presentations of frontotemporal dementia [5] and later classified as the semantic variant of primary progressive aphasia by Gorno-Tempini et al. [6]. From a clinical standpoint, patients suffering from svPPA with prevalent involvement of the left hemisphere (left svPPA) usually present with severe anomia, word-finding difficulties, and impaired single word comprehension (so-called *loss of memory for words*) [7–9]. In the case of the right hemispheric variant (right svPPA), the patients typically present with defective recognition of familiar and famous faces [10,11]. This is often in addition to bizarre food choices, food restrictions, and eating preferences (rather than binge eating, which is typical of bvFTD) [12–14]. Abnormal interests in jigsaw puzzles and clockwatching have also been reported [15]. In addition, there is a growing body of research about the behavioral alterations often exhibited by svPPA patients [16–20]. Clinico-pathological studies have shown that FTLTAR-DNA binding protein (FTLD-TDP) is the underlying pathology in about 68–80% of clinically diagnosed individuals with svPPA [21–23].

The neurodegeneration process of svPPA is known to progressively involve bilateral temporal lobes, as confirmed by a large amount of imaging studies, showing coherent patterns of structural/functional abnormalities in the brain involving the temporal poles (TPs) [16,24–33], hippocampal and parahippocampal structures [24,25,28,29,32] and the anterior inferior, middle and superior temporal gyri (aITG, aMTG and aSTG) [16,24–26,28,29,31,33,34]. As the disease progresses, the neurodegeneration may reach additional limbic regions, such as amygdala [16,25,28,29,31,33,34], the insular complex [16,28,29,31,32,34], the ventromedial prefrontal cortex (mainly orbitofrontal; vmPFC, OFC) [16,25,28,29,31,32,34] and the cingulate cortex [32]. Sometimes the basal ganglia (caudate nuclei [25,29]) are also involved. White matter alterations have been found to mirror temporal lobe grey matter abnormalities, mainly affecting inferior longitudinal and uncinate fasciculi integrity [24,35–37]. Recent works have also highlighted decreased functional connectivity in caudate nucleus and FFG [38,39].

Since the first landmark studies [40,41] ^{18}F -FDG-PET functional investigations have provided consistent findings of bilateral hypometabolism in temporal lobes, peaking in the TPs, and usually prevalent to the left [24,42–48]. Some authors have reported an additional involvement of the basal ganglia (caudate nucleus), thalamus [42,43,45], subcallosal gyrus/orbitofrontal cortex (SCG, OFC) [24,42,44,46], insula [42,49], anterior cingulate cortex (aCG) [50], and fusiform gyrus (FFG) [24,43,44,46,47].

It is of note that these findings are mostly based on group-analysis or case reports and none of them resulted from optimized voxel-based procedures applied at the single-subject level. Despite the value of parametric group-based investigations, it would be useful to develop single-subject analysis routines for clinical purposes. Therefore, our goal here is to demonstrate the value of a single-subject ¹⁸F-FDG-PET assessment in detecting functional abnormalities of glucose metabolism and their relation with the cognitive and behavioral disturbances in each svPPA patient. This could prove to be useful in clinical practice for differential and early diagnosis, especially in the case of patients with atypical presentations.

The aims of this work are: 1) To contribute a study with ¹⁸F-FDG-PET imaging using an optimized statistical parametric mapping (SPM) procedure at the single-subject and group-level in a cohort of clinically diagnosed svPPA [6]; 2) To test the correlation of performance in semantic tasks with specific brain metabolic alterations; 3) To evaluate the relationship between ¹⁸F-FDG-PET metabolic patterns as shown by SPM-t maps and CT atrophy.

Additionally, in a subgroup of patients we could test the status of white matter in the uncinate and inferior longitudinal fasciculi (UF and ILF) and their relationship with ¹⁸F-FDG-PET metabolic patterns. This is relevant given the involvement of these pathways in svPPA neurodegeneration, cognitive and behavioral disturbances.

Participants

The cohort included 10 patients (N = 4 males), mean age 67.00, standard deviation (SD) 9.13, age range 58–85, mean education 11.40 years; SD 3.92; range 5–17. They all fulfilled the criteria for svPPA [6]. The mean age at onset was 64.10; SD 10–07 (range 53–82). All the patients were evaluated at the San Raffaele Hospital (Milan, Italy) between April 2009 and July 2013 (¹⁸F-FDG-PET time) or at the IRCCS BESTA Foundation, Milan, Italy. One of the patients exhibited a novel missense progranulin gene mutation, which was described in a previous work [51]. All patients underwent a neurological examination, ¹⁸F-FDG PET/CT scan, and a detailed neuropsychological assessment. Three patients also underwent MRI Diffusion Tensor Imaging acquisition. All patients were right-handed. For a demographic summary see Table 1.

Methods

Cognitive Assessment

The cognitive evaluation was based on a detailed neuropsychological battery. This included tests for language (Token Test) [52,53] reasoning (Raven Colored Progressive Matrices [54], letter and category fluency test, [55]), short-term verbal memory (Digit Span Forward, [56] or

Table 1. Demographic summary of the studied cohort.

| Index | svPPA (9 L>R, 1 R>L) |
|------------------------|-----------------------|
| MMSE | 24.29±3.40 (18–28.27) |
| Age (yrs) | 67.00±9.13 (56–85) |
| Age at onset (yrs) | 64.10±10.07 (53–82) |
| Disease Duration (yrs) | 2.95±1.42 (0.5–4) |
| Years of Education | 11.40±3.92 (5–17) |

Statistics are indicated as follows: Mean ±SD (RANGE)

L>R: Left Hemisphere hypometabolism Asymmetry

R>L: Right Hemisphere hypometabolism Asymmetry

doi:10.1371/journal.pone.0120197.t001

Rey-Auditory Verbal Learning Test, RAVLT immediate [57], visuo-spatial short-term memory (Corsi Test [56]), verbal long-term memory (RAVLT, delayed recall [57]), long-term visual spatial memory (Rey-Osterrieth Complex Figure recall [58]), visuoconstructive abilities (Rey-Osterrieth Complex Figure copy [58]), and attention (Attentive Matrices, [53]). Furthermore, patients underwent a specific test addressing semantic processing, namely the Pyramids and Palm Trees Test [59], a widely used tool for non-verbal semantic knowledge [60]. Patients underwent also a language test developed in our center which investigates semantic memory through Confrontation Naming and Comprehension tasks [61]. As quantitative neuropsychiatric assessments were not available, this aspect was assessed on the basis of clinical records information.

¹⁸F-FDG-PET imaging

Acquisition. All subjects underwent an ¹⁸F-FDG-PET imaging session, using 3D PET scans, either a General Electric Discovery LS PET/CT or a multi-ring General Electric Discovery STE PET/CT at the Department of Nuclear Medicine, San Raffaele Hospital, Milan, Italy. Patients received an intravenous injection of approximately 270 MBq of ¹⁸F-FDG (mean dose 250,60 MBq; SD: 56,41 range 179–351) in rest condition, lying supine in a quiet, dimly-lit room. Image acquisition started approximately 45min after injection, with a scan duration of 15 minutes. In particular, before radiopharmaceutical injection of ¹⁸F-FDG, subjects were fasted for at least 6 hours and measured blood glucose level threshold of <120 mg/dL. Image reconstruction followed an ordered subset expectation maximization (OSEM) algorithm. CT was co-registered and used for attenuation correction. Scatter correction was applied with software integrated in our scanner. The protocol has been approved by the San Raffaele Hospital Local Ethical Committee. All the patients gave informed written consent.

Single-subject analysis. Image analysis was carried out with SPM5 software (Wellcome Department of Imaging Neuroscience, London, UK; www.fil.ion.ucl.ac.uk/spm) on MATLAB 8 (MathWorks Inc, Sherborn, Mass). At the single subject level, ¹⁸F-FDG-PET imaging analysis has been performed according to an optimized SPM FDG-PET pipeline previously developed and validated [62]. In a first step, scans were ‘spatially normalized’ in accordance to a reference FDG-PET “dementia-specific” template [63].

In a second step, spatially normalized and smoothed images for a single patient were then compared to a large group of control scans by means of a two-sample t-test implemented in SPM5 to assess areas of hypometabolism throughout the whole-brain at a single-subject level. Proportional scaling was used to remove intersubject global variation in PET intensities. The threshold for assessing hypometabolism was set at $p = 0.05$, FWE-corrected for multiple comparisons at the voxel level. Only clusters containing more than 100 voxels were deemed to be significant. The resulting single-subject SPM hypometabolic maps have been also visually inspected by a team of experts (neurologists, radiologists, and nuclear medicine physicians) in PET imaging in order to further validate svPPA pathologically hypometabolic areas in each patient.

Group and commonalities analysis. We also assessed hypometabolism at the group-level evaluating: (1) group differences by means of a two-sample t-test between the group of svPPA patients vs. a subset of age-matched control subjects (i.e. $N = 50$: 5 HC/1 subject). A Family Wise Error threshold of $P_{FWE} < 0.05$ was applied in order to correct for multiple comparisons (cluster extent = 100 voxels) and (2) common areas of hypometabolism in the svPPA group using the contrast images resulting from each first-order single-subject assessment. For the latter, we used a one-sample t-test, setting age as a nuisance variable. The p-value (uncorrected)

was lowered to $p < 0.001$ and the minimum cluster size was of 100 voxels, given the small number of patients.

ROI-based correlation analysis. Correlation analysis was carried out with MarsBar toolbox [64] for SPM5 software, in a one-sample t-test design, using the single-subject hypometabolism contrast images (2ND level analysis) and a covariate with confrontation naming test performances. We hypothesized the presence of a negative correlation, meaning that a greater level of decreased metabolism would correlate with a highly impaired performance. As one patient (Case 5) was tested with a naming task from a different battery (BADA, [65]), we used as covariate a vector containing a ratio between number of correct answers and maximum scores of the adopted tests. The ROIs analysis was run by selecting *a priori* a group of ROIs known to be associated with naming tasks in svPPA, together with regions commonly found hypometabolic in this condition. More specifically, we included the left temporal lobe (subdivided into ITG, MTG and STG), the FFG, IPL, caudate, amygdala and thalamus. Structural ROIs were obtained with the Wake Forest University PickAtlas (WFUPickAtlas) toolbox [66], using the Automated Anatomical Labeling (AAL) template [67] for SPM. Only individual clusters with a significance of $P_{\text{uncorrected}} < 0.05$ were deemed as significant.

CT-PET imaging

Since a CT/PET scan was performed (see descriptions in [PET imaging](#) methods section) for attenuation correction, we evaluated the CT images for presence of atrophy. An experienced board certified neuroradiologist (DP) blind-rated the atrophy levels in the CT scans (4 atrophy levels in different brain regions: none, low, mild/moderate, high/severe).

MRI Diffusion Tensor Imaging

Acquisition. A subgroup of patients ($N = 3$) and $N = 20$ age-matched healthy controls underwent a Diffusion Tensor Imaging (DTI) scan, which was performed with a 3-T Philips Achieva scanner (Philips Medical Systems, Best, NL) with an 8-channel head coil. Whole-brain DTI data was collected using a single-shot echo planar sequence (TR/TE = 8986/80 msec; FOV = 240 mm²; 56 sections; 2.5 mm isotropic resolution) with parallel imaging (SENSE factor, R = 2.5) and diffusion gradients applied along 32 non-collinear directions (b-value = 1000 sec/mm²). One non-diffusion weighted volume was also acquired.

Preprocessing and probabilistic tractography. Preprocessing and analysis of DTI data were performed via the FMRIB Software Library (FSL: <http://fsl.fmrib.ox.ac.uk/fsl/fslwiki/>) tools. Single-subject datasets were first corrected for eddy current distortions and motion artifacts, applying a full affine (linear) alignment of each volume to the no-diffusion weighting image.

We had *a priori* hypothesized the involvement of the inferior longitudinal fasciculus (ILF) and uncinate fasciculus (UF) in patients with svPPA, given the clinical features (naming difficulties and neuropsychiatric manifestations) and the abnormalities observed in ¹⁸F-FDG-PET result maps. Thus, we performed probabilistic tractography of the bilateral UF and ILF on 3 svPPA patients and 20 healthy controls, in order to test for possible fractional anisotropy (FA) and mean diffusivity (MD) changes in the fiber tracts of interest.

We used bedpostX/probtrackX to perform the multi fiber probabilistic tractography approach as described by Behrens et al. (2003, 2007) [68,69]. Both seed and termination cortical masks used to reconstruct the ILF (occipital and temporal poles) and the UF (temporal and frontal poles) were derived from the Harvard-Oxford Cortical and Subcortical Structural Atlas (<http://fsl.fmrib.ox.ac.uk/fsl/fslwiki/Atlases>).

Generated pathways are volumes in which values at each voxel represent the number of samples passing through that voxel and, therefore, the probability of connection to the seed voxel.

To remove spurious connections, the pathways in individual subjects were thresholded at 1% of the total number of generated tracts. The resulting thresholded tracts were then visually inspected to confirm that the pathways appeared anatomically correct, with no voxels outside of the expected pathway. Pathways in each subject were then binarized and averaged to produce a population probability map for each pathway. Voxel values in these maps mirror the proportion of subjects in whom a pathway is present. Group pathways were thresholded to include voxels present in at least 10% of participants and binarized to define a mask of each tract of interest.

In order to compare microstructural integrity between each single patient and the control group, we extracted mean values of FA and MD from each pathway and each subject. In particular, we employed *fslmeans* to mask the FA and MD whole-brain images with the probability maps of the ILF and UF. This allowed us to obtain mean values in all subjects for each pathway and measure. Finally, single patients' values were compared to either the 5th percentile (FA index) or the 95th percentile (MD index) of the controls' values distribution.

Results

Cognitive Assessment. Deficits in confrontation naming and/or categorical verbal fluency were present in all patients. This was associated with a relative sparing of phonemic fluency scores, a feature which has been considered as typical of svPPA, particularly in the early stages of the progression [70]. The non-pathological MMSE mean score (24.29; SD = ± 3.40) is consistent with the literature [30,71]. Six out of ten patients underwent the PPT semantic memory test and four presented with a pathological score. To summarize, a prominent disorder of semantic memory, as shown by defective performance in tests like categorical fluency, naming or word-picture matching, was found in all the patients. With a few exceptions (3/10, Case 1, 4 and 8), we found a relative sparing of the other cognitive domains (e.g. attention or visuo-constructive abilities). RAVLT testing data was available for 6/10 patients. Pathological performance at immediate recall subscore was shown by 3/6 patients, whereas 5/6 had impaired delayed recall subscores. Case 10 reported impaired recognition of her relatives on several occasions, therefore showing signs of prosopagnosia (suspected right variant svPPA). Overall the pattern of cognitive alteration was very consistent and is shown in [Table 2](#).

¹⁸F-FDG PET imaging

Single-subject analysis. Each patient showed unilateral or bilateral involvement of temporal poles (with varying degrees of asymmetry, see [Fig. 1A](#)), with additional extension to the left lateral temporal (inferior, middle and superior temporal gyrus and inferior fusiform gyrus) and medial temporal lobe regions (hippocampal formations). More specifically, in the left hemisphere, we found hypometabolism in the subiculum (7/10 patients), entorhinal cortex (5/10), and hippocampus proper (CA, 4/10). In the right hemisphere, we found metabolic decreases in fewer cases, namely 3/10 patients in the subiculum, 2/10 at entorhinal cortex and 4/10 in CA. Single-subject SPM t-maps evaluation revealed additional regional hypometabolism in limbic structures (i.e. insula, amygdala, ACG or OFC) of 8/10 patients and in IPL and temporo-parietal junction (TPJ) of 6/10. Case 10 showed an asymmetrical hypometabolism pattern prevalent in the right temporal lobe, consistent with her clinical presentation.

Group analysis. (1) Group-differences confirmed the bilateral involvement of the TPs (TP cluster significant at $P_{FWE} < 0.05$) and an extended hypometabolism in the left temporal lobe

Table 2. Neuropsychological testing results from the 10 cases presented.

| | Cut-off Score | Case 1 | Case 2 | Case 3 | Case 4 | Case 5 | Case 6 | Case 7 | Case 8 | Case 9 | Case 10 |
|------------------------|---------------|--------|--------|--------|--------|--------|--------|--------|--------|--------|---------|
| MMSE | >24 | 29* | 27.53 | 24.49 | 28,27 | 18 | 23,53 | 21.20 | 20.86 | 24.85 | 27* |
| Token Test | >29.25 | 27.25 | 34 | 31.25 | 25,75 | 23 | 29.75 | 17.5 | 16.25 | 34 | 31.25 |
| Digit Span Forward | >4.25 | 6.5 | 4 | 5.75 | 6.29 | Path° | 5.23 | 5.75 | 3.25 | 6.99 | 4.87 |
| Corsi Test | >4.25 | 4 | 5.25 | 3.75 | - | Norm° | 3.25 | 4 | 3.25 | 5.94 | 4.87 |
| RAVLT (immediate) | >28.53 | - | 21.3 | 26.4 | 20.4 | - | - | - | 30.9 | 30.3 | 42.1 |
| RAVLT (recall) | >4.69 | - | 1.7 | 2 | 2.2 | - | - | - | 3.6 | 1.8 | 9.3 |
| Naming (CAGI) | >43.99 | 14.21 | 31.21 | 12.21 | 12.287 | Path§ | 36.41 | 8 | 17.82 | 35.05 | 37.23 |
| Comprehension (CAGI) | >47.39 | 41.927 | 48 | 44.979 | 43.083 | Path§ | 48 | 36 | 44.018 | 48 | 46.018 |
| Phonemic Fluency | >23 | 17 | 34 | 27 | 21 | 0 | 22 | 0 | 26 | 27 | 13* |
| Semantic Fluency | >30 | 11 | 18 | 8 | 31 | 9 | 19 | 0 | 11 | 23 | 16* |
| Palm and Pyramids Test | >40.15 | 22** | 37 | 26** | 37.47 | - | - | 16** | - | - | 27.66 |
| | >18** | | | | | | | | | | |
| Rey Figure (Copy) | >30.05 | 28.5 | 34 | 31.25 | 21.5 | Norm° | 30.5 | 37.5 | 34.25 | 34.54 | 36 |
| Rey Figure (Recall) | >11.23 | 16.25 | 12 | 14.75 | 12.25 | - | 12.75 | 17.5 | 19.5 | 0 | 19 |
| Raven Matrices | >23.25 | 34 | 37 | 22.5 | 34 | 24.3 | 27.5 | 30.5 | 29.5 | - | 21* |
| Attentive Matrices | >37 | 46 | 46.25 | 49 | 41.25 | 49.4 | 41.75 | 41.25 | 28.50 | 37.75 | 40.75 |

All tests scores are corrected referring to respective Italian normative data (see [methods](#)).

*: These are raw scores, as it was not possible to correct scores for Years of Education and Age.

** : These scores refer to a modified version of the PPT.

§: This patient underwent similar naming and comprehension tests from a different battery (BADA); see text for details.

°: Numeric scores were not available.

Bold scores are pathological.

doi:10.1371/journal.pone.0120197.t002

(inferior, medial and antero-supero-lateral aspects). This was together with a significant involvement of the OFC (see [Table 3](#) for details) for the svPPA subjects with respect to the age-matched group of controls. (2) In the svPPA group, we found a common extensive hypometabolic cluster in the left hemisphere. This involved the inferior and middle temporal regions, insula, anterior cingulate regions. In addition, the OFC was significantly hypometabolic ($p < 0.001$ uncorrected, see [Fig. 1B](#) and [Table 3](#) for details).

ROI-based analysis. Correlation analyses showed significant negative correlation between naming task scores and hypometabolism in the left ITG (p -value < 0.045), STG (p -value < 0.009), FFG (p -value < 0.017) and caudate nucleus (p -value < 0.009) (see [Table 4](#) and [Fig. 1C](#)).

Structural imaging

CT ratings. Atrophy ratings confirmed a moderate to severe atrophy in the left TP, left anterior STG, and in left insula in more than 50% of the sample. No atrophy was reported for FFG and OFC. Mild atrophy was reported in the left frontal operculum for 30% of the patients. Left medial temporal regions (hippocampal and parahippocampal structures) were atrophic in all the patients (60% mild atrophy, 40% moderate atrophy). No atrophy was evident in the right hemisphere.

MRI DTI imaging. Probabilistic tractography revealed a lower MD index in the ILF in all 3 cases, while in the UF in 2/3 patients. FA index showed abnormal values in both UF and ILF in all the subjects (see [Table 5](#) for details).

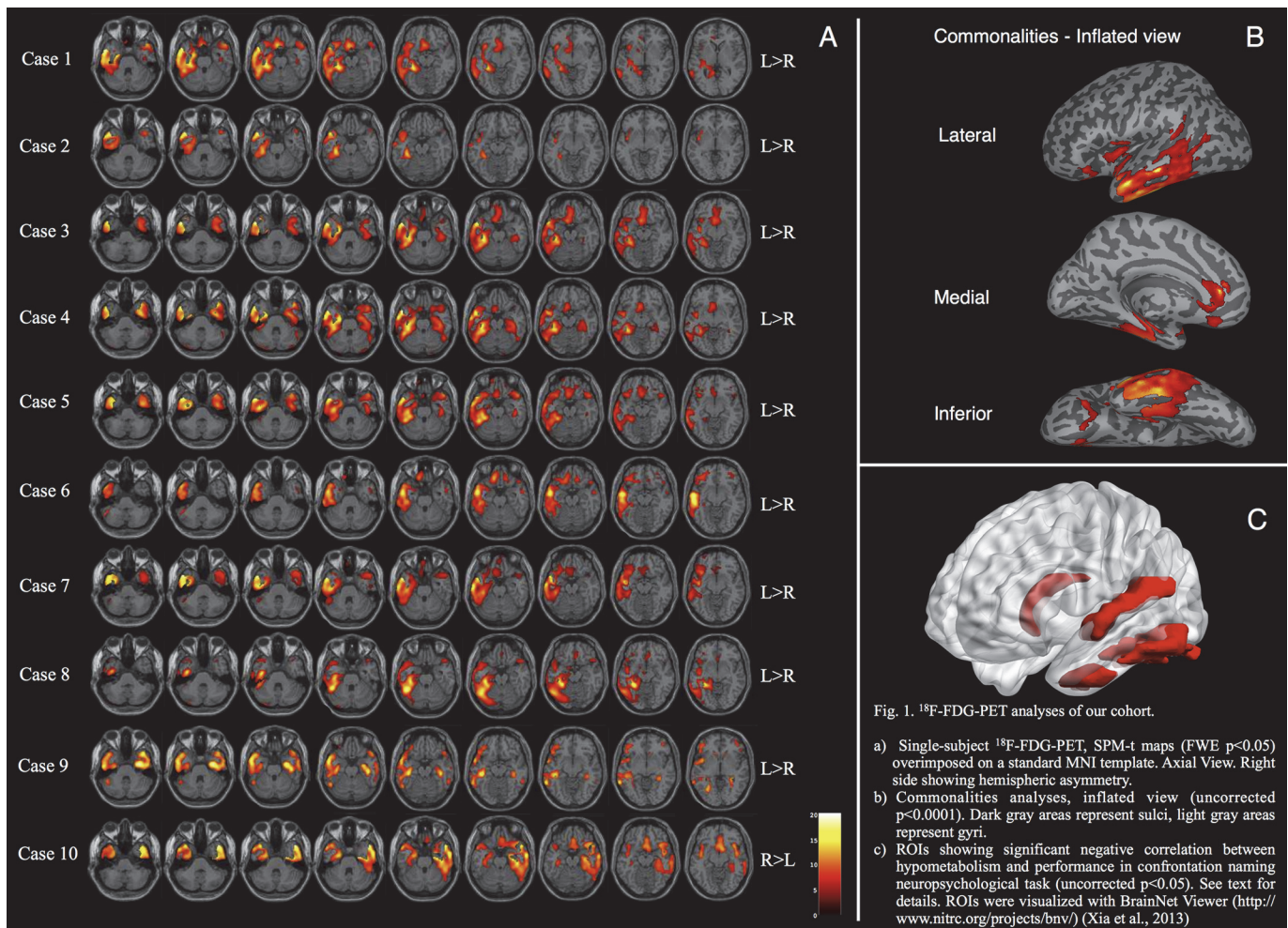


Fig 1. ¹⁸F-FDG-PET analyses of our cohort. **A)** Single-subject ¹⁸F-FDG-PET, SPM-t maps (FWE $p < 0.05$) overimposed on a standard MNI template. Axial View. Right side showing hemispheric asymmetry. **B)** Commonalities analyses, inflated view (uncorrected $p < 0.0001$). Dark gray areas represent sulci, light gray areas represent gyri. **C)** ROIs showing significant negative correlation between hypometabolism and performance in confrontation naming neuropsychological task (uncorrected $p < 0.05$). See text for details. ROIs were visualized with BrainNet Viewer (<http://www.nitrc.org/projects/bnv/>) [104].

doi:10.1371/journal.pone.0120197.g001

Discussion

Our svPPA cohort showed a prominent deterioration of semantic memory, which is the typical sign of this neurodegenerative syndrome. The preservation of executive-attentive abilities shown by svPPA patients suggests that semantic fluency difficulties may be accounted for by loss of semantic vocabulary rather than by executive deficits [71]. Verbal and spatial short-term memory domains were generally spared in our cohort (only 2/10 patients performed pathologically). The core criteria for a diagnosis of svPPA are the naming difficulties associated with deficits in single-word comprehension [6]. The confrontation naming test [61] was the most efficient tool in revealing the core semantic difficulties of svPPA patients. Single-word comprehension deficits were shown in 7 out of 10 patients. In the early stages of the disease, defective comprehension may be present only for low frequency words, leading to an underdiagnosis of the condition [22,72].

Table 3. ¹⁸F-FDG-PET group and commonalities SPM analyses.

| Analysis | P-value | MNI coordinates (x,y,z) | T | K | Label |
|--------------------------|------------------------------------|-------------------------|-------|------|---------------------|
| (1) Group | P_{FWE}<0.05 | -52,8,-26 | 12.39 | 4677 | Temporal_Mid_L |
| | | | | | Fusiform_L |
| | | | | | Temporal_Inf_L |
| | | | | | Temporal_Pole_L |
| | | 52,18,-22 | 8.56 | 544 | Parahippocampal_L |
| | | | | | Temporal_Pole_Sup_R |
| | | | | | Fusiform_R |
| | | | | | Temporal_Inf_R |
| (2) Commonalities | P_{UNCORR}<0.001 | 0,24,-18 | 7.25 | 439 | Rectus_L |
| | | | | | -8,40,10 |
| | | Temporal_Mid_L | | | |
| | | Rolandic_Operculum_L | | | |
| | | Temporal_Inf_L | | | |
| Temporal_Pole_L | | | | | |

Location, T-value and cluster size (K) of peaks of significant hypometabolism in svPPA group, divided by means of analysis approach. Labels are obtained by WFUPickAtlas SPM5 Toolbox. See [Methods](#) in text for details.

doi:10.1371/journal.pone.0120197.t003

The group analysis of ¹⁸F-FDG PET yielded results consistent with the available literature [24,42–44,47], showing selective hypometabolism in the anterior temporal lobes (TPs bilaterally), medial temporal lobes, the lateral inferior temporal cortex, extending to the temporo-occipital junction, and the limbic structures (insula, OFC and anterior cingulate region) (see [Table 2](#) and [Fig. 1B](#)).

The CT ratings confirmed a significant loss of gray matter in ATL regions, particularly in the temporal pole (on the left side) and at the medial temporal aspects level. No atrophy was revealed in FFG, confirming previous evidence (see, among the others, [24,32]). The partial discordance between the metabolic derangement and the gray matter loss may be accounted for by neural disconnection induced by early pathological events occurring in svPPA, particularly in the ATLS. The integrity of the connections seeding from these areas and projecting to frontal and posterior associative areas (through UF and ILF, respectively) appears to be altered, as shown in the patients who underwent MRI-DTI. This system disconnection and the consequent neuronal dysfunctions seem to be at the basis of the cognitive and behavioral alterations exhibited by the patients.

Table 4. Table showing ROIs significantly correlated to Confrontation Naming Test percentages scores.

| Hypothesis | Analysis | Region | P-value | x | y | z |
|---|------------------|--------|---------|-----|-----|-----|
| Negative correlation between Hypometabolism and Confrontation Naming Tests | ROI-based | L_ITG | <0.045 | -50 | -29 | -25 |
| | | L_STG | <0.009 | -53 | -22 | 6 |
| | | L_FFG | <0.017 | -40 | -48 | -22 |
| | | L_CAU | <0.009 | -12 | 10 | 8 |

Significance was set at P uncorrected <0.05. Structural Regions of Interest were extracted by normalized and published ATLAS (see text for details). P-values and coordinates are relative to the activation peaks of each ROI (see also [Fig. 1C](#)).

doi:10.1371/journal.pone.0120197.t004

Table 5. Probabilistic Tractography Results.

| ProbabilisticTractography | A – FA mean values | HC (mean) | HC (St. Dev) | HC (5 th Percentile) | Case 1 | Case 3 | Case 10 |
|---------------------------|--------------------|-----------|--------------|----------------------------------|---------------------|---------------------|---------------------|
| | Right UF_FA | 0.354044 | 0.022527 | 0.313960 | 0.321478 | 0.368426 | 0.268635* |
| | Left UF_FA | 0.355275 | 0.022342 | 0.323846 | 0.318266* | 0.34695 | 0.281353* |
| | Right ILF_FA | 0.401055 | 0.019568 | 0.369104 | 0.366063* | 0.368585* | 0.323986* |
| | Left ILF_FA | 0.409574 | 0.020515 | 0.373823 | 0.38536 | 0.372257* | 0.328735* |
| | B – MD mean values | HC (mean) | HC (St. Dev) | HC (95 th Percentile) | Case 1 | Case 3 | Case 10 |
| | Right UF_MD | 0.000880 | 0.000048 | 0.000972 | 0.000999592* | 0.000917813 | 0.00118558* |
| | Left UF_MD | 0.000862 | 0.000041 | 0.000939 | 0.00107492* | 0.00104544* | 0.00103267* |
| | Right ILF_MD | 0.000851 | 0.000033 | 0.000909 | 0.000945382* | 0.000879776 | 0.00112745* |
| | Left ILF_MD | 0.000839 | 0.000031 | 0.000891 | 0.00101494* | 0.000986195* | 0.000982657* |

A) mean FA values and B) mean MD values extracted from the bilateral uncinate fasciculus and the bilateral inferior longitudinal fasciculus. From left to right, columns indicate mean values in control group, standard deviation in control group, 5th percentile (FA: lower FA, lower white-matter integrity) or 95th percentile (MD values: higher the MD index, greater the microstructural degeneration) of the distribution of microstructural indices in healthy controls, values of case 1, values of case 3, values of case 10. Patients' values being lower than the 5th percentile (FA) or higher the 95th percentile (MD) of the distribution healthy controls' values are marked in red.

* marks significant values.

doi:10.1371/journal.pone.0120197.t005

Consistent with the naming and comprehension deficits, all the patients showed, at a single-subject level, a functional derangement encompassing the left temporal lobe, particularly in its anterior (temporal pole, superior temporal gyrus) and lateral inferior components (ITG and FFG). We further tested for associations between naming performances and hypometabolism, observing that the glucose metabolism in left ITG, STG, FFG and caudate nucleus correlated with confrontation naming scores. Significant correlations between naming scores and temporal lateral hypometabolism in svPPA have also been highlighted in previous works [28,46]. The role for the infero- and superior-lateral aspects of ATL, namely the ITG and STG, as a crucial hub in language lexical retrieval has been recently suggested by Mesulam [22]. The author claims that svPPA atrophy “challenges current concepts related to the neurology of language” and, therefore, that the left ATL should be considered as a third hub with a critical role within the language network [22]. Moreover, ITG and FFG are parts of the ‘basal temporal language area’ [73], which has a critical role in object naming and semantic processing. This region is part of the ventral stream, as shown by functional and structural imaging in both svPPA cohorts [28,32,46,74] and healthy controls [75–79]. Additionally, our analysis revealed a role for the left caudate. Some studies have already provided evidence for gray matter loss at caudate level in svPPA patients [25,29]. The negative correlation between caudate/FFG hypometabolism and naming performance might reflect a control role of the left caudate-left FFG circuit [80]. There is multiple evidence for a role of this circuit in suppressing words' production in reading tasks in bilingual settings [81,82]. Several other studies have provided evidence for a role of the caudate nucleus in several language tasks, from phonological processing [83] to word generation [84]. Case 10 is of particular interest, as this patient showed a right hemispheric dysfunction, loss of memory for words, and a remarkable prosopagnosia (she was not able on several occasions to recognize her relatives). This cognitive alteration in early stages of the disease is typical of the right variant svPPA, and our single-subject ¹⁸F-FDG-PET analysis showed a predominant metabolic dysfunction in the right temporal pole, superior temporal

gyrus and of the OFC (see [Fig. 1A](#)). The OFC cortex involvement was also coherent with irritability and mood deflections reported in the clinical history.

The single-subject ^{18}F -FDG PET analyses also revealed a consistent hypometabolism of the medial temporal lobes, precisely in the entorhinal cortices, hippocampal subiculum or CA (see [Results](#) for details). Coherently, some of our patients showed a defective performance in long-term verbal memory (RAVLT delayed recall), a finding associated with damage to specific regions of the hippocampal formation [85,86]. The defective performance on episodic verbal memory task can, at least, in part, be accounted for by the language impairment. The notion of relative preservation of episodic memory in svPPA, and of the corresponding neural correlates, is currently the focus of intensive investigation [87–89].

It is noteworthy that 80% of svPPA cases showed hypometabolism in limbic regions such as the amygdala, insula or OFC. All these patients presented with a history of neuropsychiatric manifestations, such as anxiety, depression or mood disturbances. A limit of this study, however, is that these behavioral disturbances were not quantified. Still, we observed that reported anxiety, agitation or mood disorders by the single patient were always coupled with regional hypometabolism at the single subject level in limbic areas. The behavioral alterations have been initially underestimated in svPPA patients, given the focus on the isolated language difficulties. These abnormalities have been subsequently highlighted [20], and it is now recognized that svPPA progression usually leads to behavioral manifestations [22]. Further studies are needed to investigate these behavioral disturbances and the neurofunctional correlates in svPPA.

Noteworthy, the functional involvement of limbic structures here shown in most svPPA individuals by ^{18}F -FDG PET suggests that the neurodegenerative process extends beyond the anterior aspects of the temporal pole. This area is heavily interconnected with other limbic regions and it is known to be a cortical convergence zone [90,91]. The temporal poles, initially considered a single area (BA 38), have recently been parceled out into several subregions on the basis of cytoarchitectonic differences [92] and connectivity-based approaches [93]. A recent resting-state fMRI study [94] evaluated the large-scale networks involving these subregions. At least four major temporal pole subregions, namely dorsal (auditory/somatosensory and language network connections), ventromedial (mainly visual networks), medial (paralimbic structures) and anterolateral (connected to default-semantic network), were delineated by this approach. In the case of the medial and anterolateral subregions, the uncinate fasciculus plays a crucial connection role and our MRI-DTI data support this. The UF is considered to be a component of the perisylvian language network [95] and has been specifically related to semantic memory retrieval [96,97]. The UF is also involved in socio-emotional processing [98]. A reduction of white matter integrity in the UF has been shown in the frontotemporal dementia spectrum, including in patients with svPPA [24,37,99,100]. Noteworthy, it has been also associated to behavioral symptoms (i.e. inhibition) [101]. In addition, the involvement of ILF—i.e., a component of the semantic ventral stream—seems also to be a prominent feature of the svPPA [37]. The ILF, connecting occipital and temporal regions, is thought to link object representations with their lexical labels [95]. It is also engaged in visual perception, face recognition, and reading [102]. More importantly, these white matter abnormalities may well contribute to the clinical presentation, and may be related to ^{18}F -FDG PET hypometabolism.

In conclusion, the neurodegeneration in the svPPA encompasses a widespread network, ranging from visual to limbic pathways, and affecting bilaterally the temporal lobes. Our findings indicate an extension of degeneration both caudally (towards TPJ and IPL), and rostrally, reaching first OFC and then fronto-medial cortex.

Conclusions

Our single-subject clinico-functional analysis highlighted the distinctive features of svPPA syndrome. We showed that convergent system abnormalities, from altered connectivity to metabolic dysfunction, characterize this degeneration and are associated with specific cognitive deficits. The alterations in the white matter connections within limbic regions, particularly through the uncinate fasciculus, might be the basis of the frontal extension of the neurodegeneration observed in this syndrome. Convergent findings from clinical assessment, structural imaging, and functional imaging in single cases are of utmost importance for both research and clinical practice. In the case of research, the study of svPPA has enormously contributed to the understanding of the neural basis of semantic memory [103]. In clinical practice, the coherence of imaging findings with patterns of cognitive alterations at single-subject level has an important supportive role for correct diagnosis and patient management. The ¹⁸F-FDG PET metabolic patterns in svPPA can help in the differential diagnosis in early disease phases, improving the definition of the 'diagnostic boundaries' [30] in the FTD spectrum.

Author Contributions

Conceived and designed the experiments: LI EC SFC DP. Performed the experiments: LI CC PADR. Analyzed the data: LI CC PADR. Wrote the paper: LI CC PADR EC LG AM FT GM SFC DP.

References

1. Tulving E. Episodic and Semantic Memory. Tulving E, Donaldson W, editors. *Organization of Memory*. New York: Academic Press; 1972. pp. 381–402.
2. Warrington EK. The selective impairment of semantic memory. *Q J Exp Psychol*. 1975; 27:635–57. PMID: [1197619](#)
3. Snowden JS, Goulding PJ, Neary D. Semantic Dementia a Form of Circumscribed cerebral atrophy. *Behav Neurol*. 1989; 2:167–82.
4. Hodges JR, Patterson K, Oxbury S, Funnell E. Semantic dementia. Progressive fluent aphasia with temporal lobe atrophy. *Brain*. 1992; 115 (Pt 6):1783–806.
5. Neary D, Snowden JS, Gustafson L, Passant U, Stuss D, Black S, et al. Frontotemporal lobar degeneration: a consensus on clinical diagnostic criteria. *Neurology*. 1998; 51:1546–54. PMID: [9855500](#)
6. Gorno-Tempini ML, Hillis AE, Weintraub S, Kertesz A, Mendez M, Cappa SF, et al. Classification of primary progressive aphasia and its variants. *Neurology*. 2011; 76:1006–14. doi: [10.1212/WNL.0b013e31821103e6](#) PMID: [21325651](#)
7. Ash S, Moore P, Antani S, McCawley G, Work M, Grossman M. Trying to tell a tale: discourse impairments in progressive aphasia and frontotemporal dementia. *Neurology*. 2006; 66:1405–13. PMID: [16682675](#)
8. Pijnenburg YAL, Gillissen F, Jonker C, Scheltens P. Initial Complaints in Frontotemporal Lobar Degeneration. *Dement Geriatr Cogn Disord*. 2004; 17:302–6. PMID: [15178941](#)
9. Thompson SA, Patterson K, Hodges JR. Left/right asymmetry of atrophy in semantic dementia Behavioral–cognitive implications. *Neurology*. *AAN Enterprises*; 2003; 61:1196–203. PMID: [14610120](#)
10. Gefen T, Wieneke C, Martersteck A, Whitney K, Weintraub S, Mesulam M-M, et al. Naming vs knowing faces in primary progressive aphasia: a tale of 2 hemispheres. *Neurology*. 2013; 81:658–64. doi: [10.1212/WNL.0b013e3182a08f83](#) PMID: [23940020](#)
11. Snowden JS. Knowledge of famous faces and names in semantic dementia. *Brain*. 2004; 127:860–72. PMID: [14985259](#)
12. Bozeat S, Gregory CA, Ralph MAL, Hodges JR. Which neuropsychiatric and behavioural features distinguish frontal and temporal variants of frontotemporal dementia from Alzheimer's disease? *Journal of Neurology, Neurosurgery & Psychiatry*. *BMJ Publishing Group Ltd*; 2000; 69:178–86.
13. Forman MS, Farmer J, Johnson JK, Clark CM, Arnold SE, Coslett HB, et al. Frontotemporal dementia: Clinicopathological correlations. *Ann Neurol*. 2006; 59:952–62. PMID: [16718704](#)
14. Seeley WW, Bauer AM, Miller BL, Gorno-Tempini ML, Kramer JH, Weiner M, et al. The natural history of temporal variant frontotemporal dementia. *Neurology*. 2005; 64:1384–90. PMID: [15851728](#)

15. Snowden JS, Bathgate D, Varma A, Blackshaw A, Gibbons ZC, Neary D. Distinct behavioural profiles in frontotemporal dementia and semantic dementia. *Journal of Neurology, Neurosurgery & Psychiatry*. 2001; 70:323–32.
16. Chan D, Fox NC, Scahill RI, Crum WR, Whitwell JL, Leschziner G, et al. Patterns of temporal lobe atrophy in semantic dementia and Alzheimer's disease. *Ann Neurol*. Wiley Online Library; 2001; 49:433–42. PMID: [11310620](#)
17. Noppeney U, Patterson K, Tyler LK, Moss H, Stamatakis EA, Bright P, et al. Temporal lobe lesions and semantic impairment: a comparison of herpes simplex virus encephalitis and semantic dementia. *Brain*. 2007; 130:1138–47. PMID: [17251241](#)
18. Rankin KP, Kramer JH, Mychack P, Miller BL. Double dissociation of social functioning in frontotemporal dementia. *Neurology*. 2003; 60:266–71. PMID: [12552042](#)
19. Rosen HJ, Perry RJ, Murphy J, Kramer JH, Mychack P, Schuff N, et al. Emotion comprehension in the temporal variant of frontotemporal dementia. *Brain*. Oxford Univ Press; 2002; 125:2286–95. PMID: [12244085](#)
20. Rosen H, Allison S, Ogar J, Amici S, Rose K, Dronkers N, et al. Behavioral features in semantic dementia vs other forms of progressive aphasia. *Neurology*. AAN Enterprises; 2006; 67:1752–6. PMID: [17130406](#)
21. Chare L, Hodges JR, Leyton CE, McGinley C, Tan RH, Kril JJ, et al. New criteria for frontotemporal dementia syndromes: clinical and pathological diagnostic implications. *Journal of Neurology, Neurosurgery & Psychiatry*. 2014; 85:865–70.
22. Mesulam M-M. Primary progressive aphasia and the language network: the 2013 H. Houston Merritt Lecture. *Neurology*. 2013. pp. 456–62.
23. Rohrer J, Geser F, Zhou J, Gennatas E, Sidhu M, Trojanowski J, et al. TDP-43 subtypes are associated with distinct atrophy patterns in frontotemporal dementia. *Neurology*. AAN Enterprises; 2010; 75:2204–11. doi: [10.1212/WNL.0b013e318202038c](#) PMID: [21172843](#)
24. Acosta-Cabronero J, Patterson K, Fryer TD, Hodges JR, Pengas G, Williams GB, et al. Atrophy, hypometabolism and white matter abnormalities in semantic dementia tell a coherent story. *Brain*. 2011; 134:2025–35. doi: [10.1093/brain/awr119](#) PMID: [21646331](#)
25. Brambati SM, Rankin KP, Narvid J, Seeley WW, Dean D, Rosen HJ, et al. Atrophy progression in semantic dementia with asymmetric temporal involvement: A tensor-based morphometry study. *Neurobiology of Aging*. 2009; 30:103–11. PMID: [17604879](#)
26. Davies RR, Halliday GM, Xuereb JH, Kril JJ, Hodges JR. The neural basis of semantic memory: Evidence from semantic dementia. *Neurobiology of Aging*. 2009; 30:2043–52. doi: [10.1016/j.neurobiolaging.2008.02.005](#) PMID: [18367294](#)
27. Edwards-Lee T, Miller BL, Benson DF, Cummings JL, Russell GL, Boone K, et al. The temporal variant of frontotemporal dementia. *Brain*. 1997; 120 (Pt 6):1027–40. PMID: [9217686](#)
28. Galton CJ, Patterson K, Graham K, Lambon-Ralph M, Williams G, Antoun N, et al. Differing patterns of temporal atrophy in Alzheimer's disease and semantic dementia. *Neurology*. AAN Enterprises; 2001; 57:216–25. PMID: [11468305](#)
29. Gorno-Tempini M-L, Dronkers NF, Rankin KP, Ogar JM, Phengrasamy L, Rosen HJ, et al. Cognition and anatomy in three variants of primary progressive aphasia. *Ann Neurol*. Wiley Online Library; 2004; 55:335–46. PMID: [14991811](#)
30. Kertesz A, Jesso S, Harciarek M, Blair M, McMonagle P. What is semantic dementia?: a cohort study of diagnostic features and clinical boundaries. *Arch Neurol*. Am Med Assoc; 2010; 67:483–9. doi: [10.1001/archneurol.2010.55](#) PMID: [20385916](#)
31. Mummery CJ, Patterson K, Price C, Ashburner J, Frackowiak R, Hodges JR. A voxel-based morphometry study of semantic dementia: relationship between temporal lobe atrophy and semantic memory. *Ann Neurol*. 2000; 47:36–45. PMID: [10632099](#)
32. Rohrer JD, Warren JD, Modat M, Ridgway GR, Douiri A, Rossor MN, et al. Patterns of cortical thinning in the language variants of frontotemporal lobar degeneration. *Neurology*. 2009; 72:1562–9. doi: [10.1212/WNL.0b013e3181a4124e](#) PMID: [19414722](#)
33. Schroeter ML, Raczkka K, Neumann J, Yves von Cramon D. Towards a nosology for frontotemporal lobar degenerations—A meta-analysis involving 267 subjects. *NeuroImage*. 2007; 36:497–510. PMID: [17478101](#)
34. Rosen HJ, Gorno-Tempini M-L, Goldman W, Perry R, Schuff N, Weiner M, et al. Patterns of brain atrophy in frontotemporal dementia and semantic dementia. *Neurology*. AAN Enterprises; 2002; 58:198–208. PMID: [11805245](#)
35. Agosta F, Henry RG, Migliaccio R, Neuhaus J, Miller BL, Dronkers NF, et al. Language networks in semantic dementia. *Brain*. 2010; 133:286–99. doi: [10.1093/brain/awp233](#) PMID: [19759202](#)

36. Schwindt GC, Graham NL, Rochon E, Tang-Wai DF, Lobaugh NJ, Chow TW, et al. Whole-brain white matter disruption in semantic and nonfluent variants of primary progressive aphasia. *Human Brain Mapping*. 2013; 34:973–84. doi: [10.1002/hbm.21484](https://doi.org/10.1002/hbm.21484) PMID: [22109837](https://pubmed.ncbi.nlm.nih.gov/22109837/)
37. Whitwell JL, Avula R, Senjem ML, Kantarci K, Weigand SD, Samikoglu A, et al. Gray and white matter water diffusion in the syndromic variants of frontotemporal dementia. *Neurology*. 2010; 74:1279–87. doi: [10.1212/WNL.0b013e3181d9edde](https://doi.org/10.1212/WNL.0b013e3181d9edde) PMID: [20404309](https://pubmed.ncbi.nlm.nih.gov/20404309/)
38. Agosta F, Galantucci S, Valsasina P, Canu E, Meani A, Marcone A, et al. Disrupted brain connectome in semantic variant of primary progressive aphasia. *Neurobiology of Aging*. 2014; 35:2646–55. doi: [10.1016/j.neurobiolaging.2014.05.017](https://doi.org/10.1016/j.neurobiolaging.2014.05.017) PMID: [24970567](https://pubmed.ncbi.nlm.nih.gov/24970567/)
39. Guo CC, Gorno-Tempini ML, Gesierich B, Henry M, Trujillo A, Shany-Ur T, et al. Anterior temporal lobe degeneration produces widespread network-driven dysfunction. *Brain*. 2013; 136:2979–91. doi: [10.1093/brain/awt222](https://doi.org/10.1093/brain/awt222) PMID: [24072486](https://pubmed.ncbi.nlm.nih.gov/24072486/)
40. McCarthy RA, Warrington EK. Evidence for modality-specific meaning systems in the brain. *Nature*. 1988; 334:428–30. PMID: [3261389](https://pubmed.ncbi.nlm.nih.gov/3261389/)
41. McCarthy R, Warrington EK. The dissolution of semantics. *Nature*. 1990; 343:599. PMID: [2304532](https://pubmed.ncbi.nlm.nih.gov/2304532/)
42. Desgranges B, Matuszewski V, Piolino P, Chételat G, Mézenge F, Landeau B, et al. Anatomical and functional alterations in semantic dementia: A voxel-based MRI and PET study. *Neurobiology of Aging*. 2007; 28:1904–13. PMID: [16979268](https://pubmed.ncbi.nlm.nih.gov/16979268/)
43. Diehl J, Grimmer T, Drzezga A, Riemenschneider M, Förstl H, Kurz A. Cerebral metabolic patterns at early stages of frontotemporal dementia and semantic dementia. A PET study. *Neurobiology of Aging*. 2004; 25:1051–6. PMID: [15212830](https://pubmed.ncbi.nlm.nih.gov/15212830/)
44. Drzezga A, Grimmer T, Henriksen G, Stangier I, Pernecky R, Diehl-Schmid J, et al. Imaging of amyloid plaques and cerebral glucose metabolism in semantic dementia and Alzheimer's disease. *NeuroImage*. 2008; 39:619–33. PMID: [17962045](https://pubmed.ncbi.nlm.nih.gov/17962045/)
45. Lauro-Grotto R, Piccini C, Shallice T. Modality-Specific Operations in Semantic Dementia. *CORTEX*. 1997; 33:593–622. PMID: [9444464](https://pubmed.ncbi.nlm.nih.gov/9444464/)
46. Mion M, Patterson K, Acosta-Cabronero J, Pengas G, Izquierdo-Garcia D, Hong YT, et al. What the left and right anterior fusiform gyri tell us about semantic memory. *Brain*. 2010; 133:3256–68. doi: [10.1093/brain/awq272](https://doi.org/10.1093/brain/awq272) PMID: [20952377](https://pubmed.ncbi.nlm.nih.gov/20952377/)
47. Nestor PJ, Fryer TD, Hodges JR. Declarative memory impairments in Alzheimer's disease and semantic dementia. *NeuroImage*. 2006; 30:1010–20. PMID: [16300967](https://pubmed.ncbi.nlm.nih.gov/16300967/)
48. Tyrrell P, Warrington E, Frackowiak R, Rossor M. Heterogeneity in progressive aphasia due to focal cortical atrophy in clinical and PET study. *Brain*. Oxford Univ Press; 1990; 113:1321–36. PMID: [2245299](https://pubmed.ncbi.nlm.nih.gov/2245299/)
49. Kim E-J, Kim BC, Kim S-J, Jung DS, Sin J-S, Yoon Y-J, et al. Clinical staging of semantic dementia in an FDG-PET study using FTLD-CDR. *Dement Geriatr Cogn Disord*. 2012; 34:300–6. doi: [10.1159/000345506](https://doi.org/10.1159/000345506) PMID: [23208196](https://pubmed.ncbi.nlm.nih.gov/23208196/)
50. Diehl J, Grimmer T, Drzezga A, Bomschein S, Pernecky R, Förstl H, et al. Longitudinal Changes of Cerebral Glucose Metabolism in Semantic Dementia. *Dement Geriatr Cogn Disord*. 2006; 22:346–51. PMID: [16954690](https://pubmed.ncbi.nlm.nih.gov/16954690/)
51. Cerami C, Marcone A, Galimberti D, Villa C, Fenoglio C, Scarpini E, et al. Novel Missense Progranulin Gene Mutation Associated with the Semantic Variant of Primary Progressive Aphasia. *Journal of Alzheimer's Disease*. IOS Press; 2013; 36:415–20. doi: [10.3233/JAD-130317](https://doi.org/10.3233/JAD-130317) PMID: [23624518](https://pubmed.ncbi.nlm.nih.gov/23624518/)
52. De Renzi A, Vignolo LA. Token test: A sensitive test to detect receptive disturbances in aphasics. *Brain*. Oxford Univ Press; 1962; 85:665–78. PMID: [14026018](https://pubmed.ncbi.nlm.nih.gov/14026018/)
53. Spinnler H, Tognoni G. Taratura e standardizzazione italiana di test neuropsicologici. *Italian Journal of Neurological Sciences*. 1987; 1:1–120.
54. Basso A, Capitani E, Laiacoma M. Raven's coloured progressive matrices: normative values on 305 adult normal controls. *Funct. Neurol*. 1987; 2:189. PMID: [3666548](https://pubmed.ncbi.nlm.nih.gov/3666548/)
55. Novelli G, Papagno C, Capitani E, Laiacoma M, Cappa S, Vallar G. Three clinical tests for the assessment of verbal long term memory function. Norms from 320 normal subjects. *Archivio di Psicologia, Neurologia e Psichiatria*. 1986; 47:278–96.
56. Orsini A, Grossi D, Capitani E, Laiacoma M, Papagno C, Vallar G. Verbal and spatial immediate memory span: normative data from 1355 adults and 1112 children. *The Italian Journal of Neurological Sciences*. Springer; 1987; 8:537–48.
57. Carlesimo GA, Caltagirone C, Gainotti G, Nocentini U. Batteria per la valutazione del deterioramento mentale (PARTE II): Standardizzazione e affidabilità diagnostica nell'identificazione di pazienti affetti da sindrome demenziale. *Archivio di Neurologia, Psicologia e Psichiatria*. 1995; 1–18.

58. Caffarra P, Vezzadini G, Dieci F, Zonato F, Venneri A. Rey-Osterrieth complex figure: normative values in an Italian population sample. *Neurol Sci*. Springer; 2002; 22:443–7. PMID: [11976975](#)
59. Gamboz N, Coluccia E, Iavarone A, Brandimonte MA. Normative data for the Pyramids and Palm Trees Test in the elderly Italian population. *Neurol Sci*. 2009; 30:453–8. doi: [10.1007/s10072-009-0130-y](#) PMID: [19768374](#)
60. Howard D, Patterson K. *The Pyramids and Palm Trees Test. A test of semantic access from words and pictures.* Bury St. Edmunds: Thames Valley Company; 1992.
61. Catricalà E, Della Rosa PA, Ginex V, Mussetti Z, Plebani V, Cappa SF. An Italian battery for the assessment of semantic memory disorders. *Neurol Sci*. 2012; 34:985–93. doi: [10.1007/s10072-012-1181-z](#) PMID: [22960873](#)
62. Perani D, Della Rosa PA, Cerami C, Gallivanone F, Fallanca F, Vanoli EG, et al. Validation of an optimized SPM procedure for FDG-PET in dementia diagnosis in a clinical setting. *YNICL*. 2014; 6:445–54.
63. Della Rosa PA, Cerami C, Gallivanone F, Prestia A, Caroli A, Castiglioni I, et al. A standardized [18F]-FDG-PET template for spatial normalization in statistical parametric mapping of dementia. *Neuroinformatics*. 2014; 12:575–93. doi: [10.1007/s12021-014-9235-4](#) PMID: [24952892](#)
64. Brett M, Anton J-L, Valabrègue R, Poline J-B. Region of interest analysis using an SPM toolbox. 8th International Conference on Functional Mapping of the Human Brain. Available on CD-ROM in *NeuroImage*, Vol 16, No 2, abstract 497. Sendai, Japan; 2002.
65. Miceli G, Laudanna A, Burani C, Capasso R. *Batteria per l'analisi dei deficit afasici.* Cepsag, Roma. 1994.
66. Maldjian JA, Laurienti PJ, Kraft RA, Burdette JH. An automated method for neuroanatomic and cytoarchitectonic atlas-based interrogation of fMRI data sets. *NeuroImage*. 2003; 19:1233–9. PMID: [12880848](#)
67. Tzourio-Mazoyer N, Landeau B, Papathanassiou D, Crivello F, Etard O, Delcroix N, et al. Automated anatomical labeling of activations in SPM using a macroscopic anatomical parcellation of the MNI MRI single-subject brain. *NeuroImage*. 2002; 15:273–89. PMID: [11771995](#)
68. Behrens T, Johansen Berg H, Woolrich M, Smith S, Wheeler-Kingshott C, Boulby P, et al. Non-invasive mapping of connections between human thalamus and cortex using diffusion imaging. *Nat Neurosci*. Nature Publishing Group; 2003; 6:750–7. PMID: [12808459](#)
69. Behrens T, Berg HJ, Jbabdi S, Rushworth M, Woolrich M. Probabilistic diffusion tractography with multiple fibre orientations: What can we gain? *NeuroImage*. Elsevier; 2007; 34:144–55. PMID: [17070705](#)
70. Marczyński CA, Kertesz A. Category and letter fluency in semantic dementia, primary progressive aphasia, and Alzheimer's disease. *Brain and Language*. 2006; 97:258–65. PMID: [16325251](#)
71. Hodges JR, Patterson K. Semantic dementia: a unique clinicopathological syndrome. *The Lancet Neurology*. 2007; 6:1004–14. PMID: [17945154](#)
72. Kertesz A, Davidson W, McCabe P, Takagi K, Munoz D. Primary progressive aphasia: diagnosis, varieties, evolution. *J Int Neuropsychol Soc*. Cambridge Univ Press; 2003; 9:710–9. PMID: [12901777](#)
73. Lüders H, Lesser R, Hahn J, Dinner D, Morris H, Wyllie E, et al. Basal temporal language area. *Brain*. Oxford Univ Press; 1991; 114:743–54. PMID: [2043946](#)
74. Mummery CJ, Patterson K, Wise RJ, Vandenberghe R, Price CJ, Hodges JR. Disrupted temporal lobe connections in semantic dementia. *Brain*. 1999; 122 (Pt 1):61–73.
75. Binney RJ, Embleton KV, Jefferies E, Parker GJM, Lambon Ralph MA. The Ventral and Inferolateral Aspects of the Anterior Temporal Lobe Are Crucial in Semantic Memory: Evidence from a Novel Direct Comparison of Distortion-Corrected fMRI, rTMS, and Semantic Dementia. *Cerebral Cortex*. 2010; 20:2728–38. doi: [10.1093/cercor/bhq019](#) PMID: [20190005](#)
76. Damasio H, Tranel D, Grabowski T, Adolphs R, Damasio A. Neural systems behind word and concept retrieval. *Cognition*. 2004; 92:179–229. PMID: [15037130](#)
77. Liljeström M, Hultén A, Parkkonen L, Salmelin R. Comparing MEG and fMRI views to naming actions and objects. Salmelin R, Baillet S, editors. *Human Brain Mapping*. 2009; 30:1845–56. doi: [10.1002/hbm.20785](#) PMID: [19378277](#)
78. Tomaszewski Farias S, Harrington G, Broomand C, Seyal M. Differences in functional MR imaging activation patterns associated with confrontation naming and responsive naming. *AJNR Am J Neuroradiol*. 2005; 26:2492–9. PMID: [16286390](#)
79. Visser M, Ralph ML. Differential contributions of bilateral ventral anterior temporal lobe and left anterior superior temporal gyrus to semantic processes. *Journal of Cognitive Neuroscience*. MIT Press; 2011; 23:3121–31. doi: [10.1162/jocn_a_00007](#) PMID: [21391767](#)

80. Crinion J. Language Control in the Bilingual Brain. *Science*. 2006; 312:1537–40. PMID: [16763154](#)
81. Ali N, Green DW, Kherif F, Devlin JT, Price CJ. The Role of the Left Head of Caudate in Suppressing Irrelevant Words. *Journal of Cognitive Neuroscience*. 2010; 22:2369–86. doi: [10.1162/jocn.2009.21352](#) PMID: [19803688](#)
82. Tan LH, Chen L, Yip V, Chan AHD, Yang J, Gao J-H, et al. Activity levels in the left hemisphere caudate-fusiform circuit predict how well a second language will be learned. *Proc. Natl. Acad. Sci. U.S.A.* 2011; 108:2540–4. doi: [10.1073/pnas.0909623108](#) PMID: [21262807](#)
83. Tettamanti M, Moro A, Messa C, Moresco RM, Rizzo G, Carpinelli A, et al. Basal ganglia and language: phonology modulates dopaminergic release. *Neuroreport*. 2005; 16:397–401. PMID: [15729145](#)
84. Vitali P, Abutalebi J, Tettamanti M, Rowe J, Scifo P, Fazio F, et al. Generating animal and tool names: An fMRI study of effective connectivity. *Brain and Language*. Elsevier; 2005; 93:32–45. PMID: [15766766](#)
85. Chen KHM, Chuah LYM, Sim SKY, Chee MWL. Hippocampal region-specific contributions to memory performance in normal elderly. *Brain and Cognition*. Elsevier Inc; 2010; 72:400–7. doi: [10.1016/j.bandc.2009.11.007](#) PMID: [20044193](#)
86. Golomb J, de Leon MJ, Kluger A, George AE, Tarshish C, Ferris SH. Hippocampal atrophy in normal aging: an association with recent memory impairment. *Arch Neurol*. American Medical Association; 1993; 50:967–73. PMID: [8363451](#)
87. La Joie R, Landeau B, Perrotin A, Bejanin A, Egret S, Pélerin A, et al. Intrinsic Connectivity Identifies the Hippocampus as a Main Crossroad between Alzheimer's and Semantic Dementia-Targeted Networks. *Neuron*. Elsevier Inc; 2014; 81:1417–28. doi: [10.1016/j.neuron.2014.01.026](#) PMID: [24656258](#)
88. Ranganath C, Ritchey M. Two cortical systems for memory-guided behaviour. *Nat Rev Neurosci*. 2012; 13:713–26. doi: [10.1038/nrn3338](#) PMID: [22992647](#)
89. Tan RH, Wong S, Kril JJ, Piguet O, Homberger M, Hodges JR, et al. Beyond the temporal pole: limbic memory circuit in the semantic variant of primary progressive aphasia. *Brain*. 2014;:1–12.
90. Binder JR, Desai RH, Graves WW, Conant LL. Where Is the Semantic System? A Critical Review and Meta-Analysis of 120 Functional Neuroimaging Studies. *Cerebral Cortex*. 2009; 19:2767–96. doi: [10.1093/cercor/bhp055](#) PMID: [19329570](#)
91. Visser M, Jefferies E, Lambon Ralph MA. Semantic processing in the anterior temporal lobes: a meta-analysis of the functional neuroimaging literature. *Journal of Cognitive Neuroscience*. 2010; 22:1083–94. doi: [10.1162/jocn.2009.21309](#) PMID: [19583477](#)
92. Blaizot X, Mansilla F, Insausti A, Constans J, Salinas-Alaman A, Pro-Sistiaga P, et al. The human parahippocampal region: I. Temporal pole cytoarchitectonic and MRI correlation. *Cerebral Cortex*. Oxford Univ Press; 2010; 20:2198–212. doi: [10.1093/cercor/bhp289](#) PMID: [20064939](#)
93. Fan L, Wang J, Zhang Y, Han W, Yu C, Jiang T. Connectivity-based parcellation of the human temporal pole using diffusion tensor imaging. *Cerebral Cortex*. Oxford Univ Press; 2013;:1–14.
94. Pascual B, Masdeu JC, Hollenbeck M, Makris N, Insausti R, Ding S-L, et al. Large-Scale Brain Networks of the Human Left Temporal Pole: A Functional Connectivity MRI Study. *Cerebral Cortex*. Oxford Univ Press; 2013;:1–23.
95. Catani M, Mesulam M. The arcuate fasciculus and the disconnection theme in language and aphasia: history and current state. *CORTEX*. Elsevier; 2008; 44:953–61. doi: [10.1016/j.cortex.2008.04.002](#) PMID: [18614162](#)
96. de Zubicaray GI, Rose SE, McMahon KL. The structure and connectivity of semantic memory in the healthy older adult brain. *NeuroImage*. Elsevier Inc; 2011; 54:1488–94. doi: [10.1016/j.neuroimage.2010.08.058](#) PMID: [20807579](#)
97. Papagno C, Miracapillo C, Casarotti A, Lauro LJR, Castellano A, Falini A, et al. What is the role of the uncinate fasciculus? Surgical removal and proper name retrieval. *Brain*. Oxford Univ Press; 2011; 134:405–14. doi: [10.1093/brain/awq283](#) PMID: [20959310](#)
98. Heide Von Der RJ, Skipper LM, Klobusicky E, Olson IR. Dissecting the uncinate fasciculus: disorders, controversies and a hypothesis. *Brain*. Oxford Univ Press; 2013; 136:1692–707. doi: [10.1093/brain/awt094](#) PMID: [23649697](#)
99. Agosta F, Scola E, Canu E, Marcone A, Magnani G, Sarro L, et al. White Matter Damage in Frontotemporal Lobar Degeneration Spectrum. *Cerebral Cortex*. 2012; 22:2705–14. doi: [10.1093/cercor/bhr288](#) PMID: [21988828](#)
100. Galantucci S, Tartaglia MC, Wilson SM, Henry ML, Filippi M, Agosta F, et al. White matter damage in primary progressive aphasias: a diffusion tensor tractography study. *Brain*. 2011; 134:3011–29. doi: [10.1093/brain/awr099](#) PMID: [21666264](#)

101. Hornberger M, Geng J, Hodges JR. Convergent grey and white matter evidence of orbitofrontal cortex changes related to disinhibition in behavioural variant frontotemporal dementia. *Brain*. 2011; 134:2502–12. doi: [10.1093/brain/awr173](https://doi.org/10.1093/brain/awr173) PMID: [21785117](https://pubmed.ncbi.nlm.nih.gov/21785117/)
102. Catani M, de Schotten MT. *Atlas of human brain connections*. Oxford University Press; 2012.
103. Patterson K, Nestor PJ, Rogers TT. Where do you know what you know? The representation of semantic knowledge in the human brain. *Nat Rev Neurosci*. 2007; 8:976–87. PMID: [18026167](https://pubmed.ncbi.nlm.nih.gov/18026167/)
104. Xia M, Wang J, He Y. BrainNet Viewer: a network visualization tool for human brain connectomics. *PLoS ONE*. 2013; 8:e68910. doi: [10.1371/journal.pone.0068910](https://doi.org/10.1371/journal.pone.0068910) PMID: [23861951](https://pubmed.ncbi.nlm.nih.gov/23861951/)